Optimization of ultrasonic cavitation processing in the liquid melt flow

IOP Conf. Series: Materials Science and Engineering **529** (2019) 012050 doi:10.1088/1757-899X/529/1/012050

Optimization of ultrasonic cavitation processing in the liquid melt flow

T Subroto[1], D G Eskin[1,2,*], I Tzanakis[3,4], G S B. Lebon[1], A Miranda[1], K. Pericleous[5]

[1]Brunel Centre for Advanced Solidification Technology, Brunel University London, Kingston Lane, Uxbridge UB8 3PH, UK
[2]Tomsk State University, Tomsk, 634050, Russia
[3]Faculty of Technology, Design and Environment, Oxford Brookes University, Oxford OX33 1HX, UK
[4] Department of Materials, University of Oxford, Oxford OX1 3PH, United Kingdom
[5]Computational Science and Engineering Group (CSEG), Department of Mathematics, University of Greenwich, London SE10 9LS, United Kingdom

Email: dmitry.eskin@brunel.ac.uk

Abstract. Ultrasonic processing (USP) during direct-chill (DC) casting of light metal alloys is typically applied in the sump of a billet. This approach, though successful for structure refinement and modification, has two main drawbacks: (a) mixture of mechanisms that rely heavily on dendrite fragmentation and (b) a limited volume that can be processed by a single ultrasonic source. We suggest moving the location of USP from the sump to the launder and applying it to the melt flow for continuous treatment. The apparent benefits include: (a) degassing of the melt volume, (b) grain refinement through activation of non-metallic inclusions, fragmentation of primary crystals, and deagglomeration of grain refining substrates, and (c) a possibility to use a single ultrasonic source for processing large melt volumes. To optimize this process with regard to the acoustic intensity and melt residence time in the active cavitation zone, flow modification with baffles as well as informed location of the ultrasonic source are required. In this paper, we demonstrate the results of experimental trials where the degassing degree and grain refinement have been the indicators of the USP efficiency for two aluminium alloys, i.e. LM25 and AA7050. The results are supported by acoustic measurements and computer simulations.

1. Introduction

Treating liquid metal with ultrasound, i.e. ultrasonic melt processing (USP), produces beneficial results that include melt degassing and structure refinement of the as-cast alloy. It is an efficient, economical, and clean melt treatment technology. For example, instead of injecting an inert or chemically inactive gas such as argon to extract hydrogen from the melt, cavitation bubbles are generated during USP and leave the melt through buoyancy when they grow due to rectified diffusion of hydrogen, i.e., a process where hydrogen diffuses into the bubble during the rarefaction acoustic cycle [1]. In the case of structure refinement, the cost of common grain refinement agents such as TiB_2 for aluminium alloys [2] or zirconium for some Mg alloys [3] could be reduced or avoided by using USP. These benefits are highly attractive for industrial applications.

Due to its current limitation in treating large melt volumes, USP is mostly confined to laboratory or small-scale processing despite its potential advantages [4]. To circumvent this problem, multiple

ultrasonic sources are utilized [1]. However, this solution reduces its economic feasibility thereby hampering its widespread industrial adoption. The imminent challenge for USP technology is to improve melt treatment efficiency at industrial scale using a single ultrasonic source.

Recent developments in USP modelling [5,6] enabled us to design a flow modification system in the launder (i.e. using various partition configurations and different sonotrode locations) that maximized the melt residence time in the cavitation active zone. In addition, such models also predicted that resonance conditions in a launder can increase the bubble concentration [7] and thus cavitation activity. Recent technological developments in cavitation intensity measurements [8] enabled us to quantify acoustic pressures and map the pressure field in the melt. These measurements allowed further numerical model development and supported the design of a smart flow modification system in the launder for optimized USP.

In this work, we verify the resonance phenomenon by varying the distance between partitions in a launder. Resonance is an attractive trait for improving USP efficiency on a single sonotrode configuration. The effect of sonotrode placement with respect to partitions is also studied. Acoustic pressures were measured in a water model. Metallurgical indicators such as degassing efficiency and grain refinement analysis were used to assess USP efficiency in the liquid metal experiments.

2. Materials and methods

2.1. Cavitation activity measurement

Acoustic pressures were measured in water with a calibrated cavitometer. A detailed description of cavitometer, data acquisition process and pressure conversion procedure has been previously described in [5, 9,10]. A 1-kW Hielscher piezoelectric ultrasonic transducer with a titanium cylindrical sonotrode (diameter 40 mm) was used in water experiments at a power of 70% (corresponding to 12 µm peak-to-peak ultrasonic tip amplitude displacement). The sonotrode tip was immersed 1 cm below the free surface.

A launder with partitions made from transparent plastic material was used to study the acoustic behaviour of water under USP. The length and width of such a launder were 100 cm and 9.4 cm, respectively. More details of this launder has been previously described in [7]. The gap between the partitions and the launder where water can flow through were 2 cm and 1 cm for upstream and downstream partition, respectively. The configuration of the partitions (flow passed below upstream partition and above downstream partition) was intended so there would be a recirculation of the liquid between the partitions. This ultimately maximizes pressures and cavitation activity to attain more inclusion activation and particle fragmentation by higher pressures and more efficient redistribution of the acoustic energy.

To observe acoustic resonance effect in water, acoustic measurements at three partition distances were carried out. The measurements were performed under the sonotrode. Two partition separation distances represent *n*-fold water wavelengths at ultrasonic frequency of 20 kHz—15 cm (2 λ_{water}) and 30 cm (4 λ_{water}), and one width (20 cm) represents an off-wavelength partition width. The effect of sonotrode placement with respect to the partitions was also studied. Three sonotrode locations were used: next to the upstream partition, next to the downstream partition, and equidistant between both partitions. Experiments were repeated with water flow (of 2 l/min) and without flow. The case corresponding to a partition separation of 15 cm is simulated using a numerical model that was validated with Particle Image Velocimetry (PIV) measurements in water [11].

2.2. Metallurgical indicator

The experiments with liquid aluminium alloys were performed in a launder made from refractory material. The length and width of such a launder were 90 cm and 10 cm, respectively. A liquid alloy was poured to the launder at a flow rate of 1 l/min. A thermocouple was placed in the vicinity of the launder exit, where samples were collected. USP was performed with a Reltec water-cooled magnetostrictive ultrasonic transducer (5 kW) operating at 17.5 kHz. A conical Nb sonotrode tip

(diameter 20 mm) was immersed 2 cm below the free surface of the melt. USP power of 3 kW corresponding to 33 µm peak-to-peak USP tip amplitude was used. The partitions were placed at 1 wavelength distance for liquid aluminium at 17.5 kHz, which is 26 cm. The experimental setup for liquid metal experiments is shown in Figure 1.

The degassing efficiency of USP process was assessed with an LM25 alloy (Al–7.5 wt% Si). This is because Al–Si alloys can have relatively high content of hydrogen in melt [12], thus may provide a clear indication of degassing efficiency. Samples were collected at different process conditions: without USP, with sonotrode at different positions while one reference sample was taken when the melt was still in the furnace. Density index (DI%) (the difference between the densities of the sample solidified under atmospheric pressure and the sample solidified under vacuum related to the density of the sample solidified under atmospheric pressure) that can be regarded as a measure of the end-cast product cleanliness was calculated from reduced pressure tests (RPT) which was performed using RPT (3VTMKGmbh) machine. At least three samples from independent experiments were obtained from each position and process conditions.

AA7050 alloy was used for assessing grain refinement efficiency of USP as it contains the necessary elements (Zr and Ti) that can trigger effective grain refinement under cavitation condition [1,13]. Three samples were collected as the melt left the launder. The samples were solidified in a TP1 mould. For this analysis, samples were obtained at different sonotrode positions and one sample obtained without USP as a reference. Standard metallographic sample preparation procedure and optical microscopy technique was utilized to measured grain size.

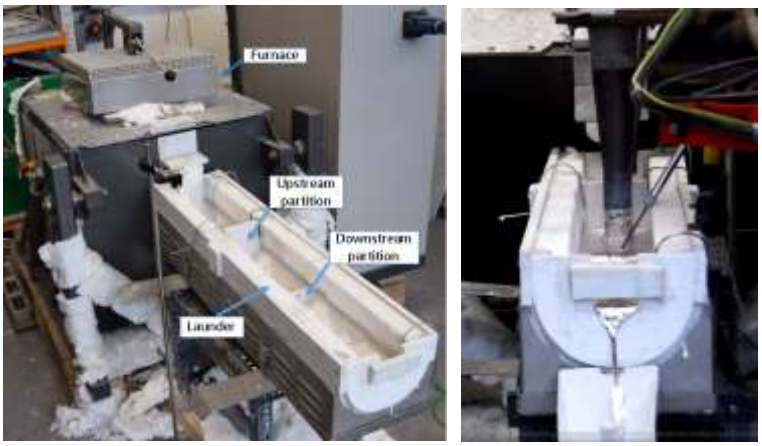

(a) (b)

Figure 1. Photos of experimental setup used for liquid metal experiments. (a) Position of furnace, launder and partitions (b) with ultrasonic sonotrode and liquid metal experiment running.

3. Results and discussion

3.1. Acoustic measurements

Figure 2a and 2b show the measured maximum and root mean square (RMS) pressures in water, respectively. The highest maximum pressure with flow was recorded when the sonotrode was positioned next to the downstream partition (1.47–1.49 MPa). The pressure at the centre position is 1.36–1.42 MPa and the lowest pressure was recorded with the sonotrode next to the upstream partition (1.24–1.38 MPa). Figure 2 also shows that the highest pressure was measured when the partition distance was $2\lambda_{water}$, and followed by $4\lambda_{water}$. The lowest pressure was obtained when the partition separation was at off-wavelength distance (20 cm). These results support the prediction that a resonance length promotes an increase in pressures [10]. This result also reveals that this resonance effect does not only occur at one liquid wavelength, but also at n-fold liquid wavelengths (where n is an integer number). According to Figure 2, the resonance effect decreases with increasing n, presumably due to attenuating pressures as the sound waves have to travel over a longer distance in a bubbly medium.

Figure 2 also shows that the presence of the flow leads to an increase in the measured acoustic pressure regardless of the position of sonotrode and the distances between partitions. In terms of maximum pressure (Figure 2a), the upstream position has the most significant pressure increase, followed by downstream position and the centre position has the least pressure increase. The trend between maximum pressure and RMS is similar on different sonotrode positions and partition distances. RMS value represents the average of maximum RMS acoustic pressure measured from 60 individual waveforms. Figure 2b shows that without flow, the RMS value is approximately less than one-fifth of the maximum pressure value, while measurements with flow produced RMS value close to 20% of the maximum pressure value. This is probably due to the decrease in the shielding effect under the sonotrode as bubbles are advected downstream. With less bubbles to surround the sonotrode surface, pressure waves can propagate more freely and over longer distances in the liquid medium with less attenuation.

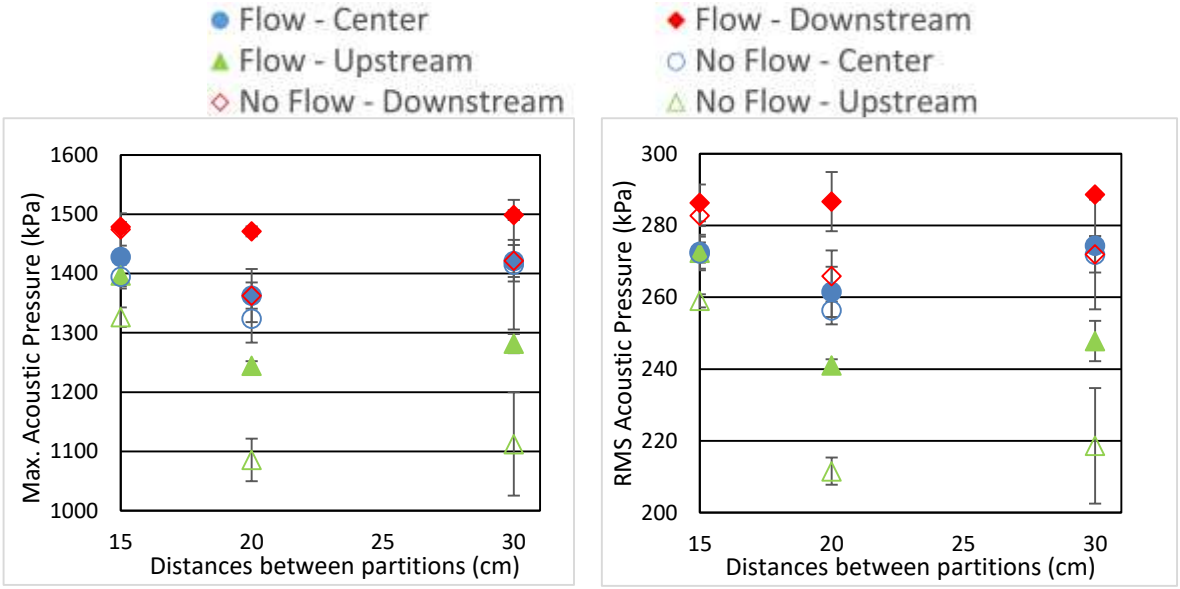

(a) (b)

Figure 2. Effect of flow in water experiments, sonotrode positions with respect to partitions (upstream, centre and downstream), and distances between partitions – comparison between n-fold λ_{water} and non-λ_{water} partition distances. (a) Maximum pressure measurements and (b) RMS measurements.

3.2. Numerical results

Figure 3 shows the predicted acoustic pressure in a 3D representation of the water launder when the sonotrode is placed centrally between the two partitions. The results show that the highest pressures are recorded downstream, in qualitative agreement with the results from the previous section. Note that these results are highly sensitive to the assumed bubble density in water, which is an unknown parameter [11]. Numerical discrepancies can be explained by the lack of knowledge of this crucial factor: an empirical validation of this crucial parameter is currently being studied.

3.3. Metallurgical indicator

Figure 4 shows the effectiveness of degassing using USP assessed using density index (DI%) parameter. Higher value represents less degassing efficiency and lower value otherwise. The positive effect of USP for degassing can be clearly seen as samples taken without USP (launder) has highest average DI index. Among three different sonotrode positions, the best degassing result is obtained when the sonotrode was positioned next to the downstream partition that is in agreement with the experimental measurements of acoustic pressure in Figure 2. The DI is higher when the sample obtained in the launder without UST compared with the one in the furnace, which is logical as there is less water vapour in the furnace, thus less hydrogen pickup by the liquid metal.

Figure 5 shows the grain refinement efficiency of USP. USP clearly promoted grain refinement with samples after USP having smaller grain size. Figure 5a suggests that the best grain refinement was achieved when the sonotrode was positioned either in the centre between partitions or nearby downstream partition, which an average grain size reduction of up to 50% as compared to upstream position or without USP. The effect of melt temperature is demonstrated in Figure 5 on two sets of data taken at different temperatures. It is clear that USP treatment temperature has a critical influence on the structure refinement outcome, as reported by previous researches [1,14]. If intermetallic fragmentation is the main mechanism for grain refinement in this type of USP, treatment at lower temperature would yield better structure refinement due to the larger presence of intermetallics and due to a higher cavitation activity.

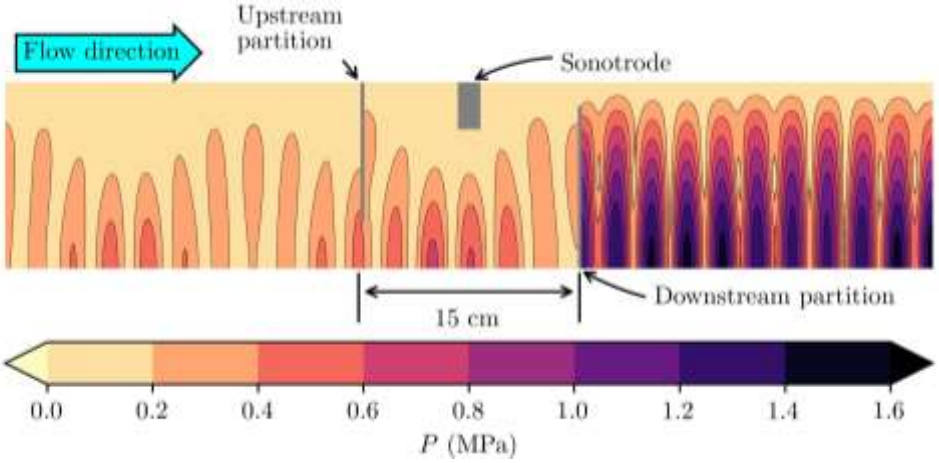

Figure 3. Predicted acoustic pressure in the water launder for a case with flowing water, representative of the experiment with distance between the partitions equal to two wavelengths of water and the sonotrode placed at the center. The aspect ratio is altered by a factor of 5.0 for clarity.

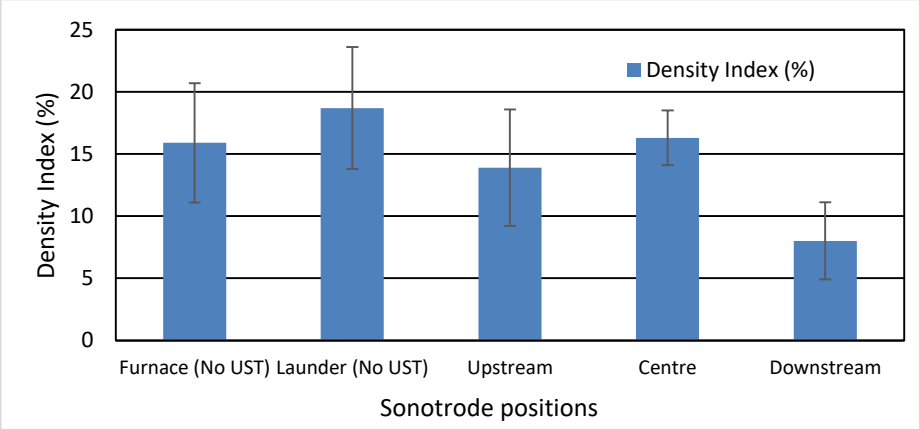

Figure 4. Density index (DI %) obtained through reduced pressure test for samples taken at different locations and processed with USP at different sonotrode positions.

From both acoustic measurements in water and liquid metals experiments, we found a coherent response. The better USP efficiency was achieved by placing the sonotrode nearby downstream partition. This corresponds to the highest acoustic pressure built up under resonance, and along with the flow pattern can increase re-circulation and residence time [14]. The second effect is the propagation of acoustic waves and cavitation activity beyond the downstream partition, which prolongs USP of the incoming melt to the downstream part of the launder. These mechanisms can ultimately improve the USP efficiency.

4. Summary

The resonance effect was observed in water experiments. Larger acoustic pressures were measured when the partition distance corresponds to integer wavelengths and lower pressures were measured when the distance is not a wavelength integer. The resonance effect does not only occur at one liquid wavelength but also at n-fold liquid wavelengths (higher-order resonance), though with attenuation.

The optimum location of the sonotrode is next to the downstream partition. This is well supported by various indicators, both from water and liquid metal experiments. The findings from this work clearly demonstrate that flow modification through variations of partition distances and placements of the sonotrode could provide improvement in USP efficiency, which could be worth to explore further for bringing the USP technology to industry.

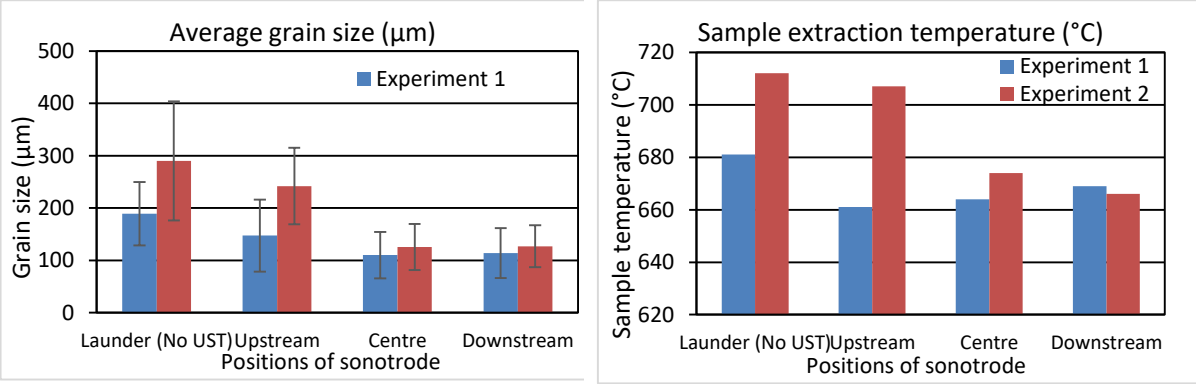

Figure 5. Structure refinement efficiency analysis from two independent experiments for samples taken at different process conditions. (a) Grain size analysis and (b) temperature where samples were obtained.

5. Acknowledgments

Financial supports from EPSRC UK through grants UltraMelt 2 (EP/R011001/1, EP/R011044/1, EP/R011095/1) and LiME Hub (EP/N007638/1) are gratefully acknowledged.

References

[1] Eskin G I and Eskin D G 2017 *Ultrasonic treatment of light alloy melts, second edition.* (CRC Press)
[2] Wang X and Han Q 2016 Grain Refinement Mechanism of Aluminum by Al-Ti-B Master Alloys *Light Metals 2016* ed E Williams (Cham: Springer International Publishing) pp 189–93
[3] Qian M and Das A 2006 Grain refinement of magnesium alloys by zirconium: Formation of equiaxed grains *Scr. Mater.* **54** 881–6
[4] Eskin D G 2017 Ultrasonic processing of molten and solidifying aluminium alloys: overview and outlook *Mater. Sci. Technol.* **33** 636–45
[5] Lebon G S B, Tzanakis I, Pericleous K and Eskin D 2018 Experimental and numerical investigation of acoustic pressures in different liquids *Ultrason. Sonochem.* **42** 411–21
[6] Lebon G S B, Tzanakis I, Djambazov G, Pericleous K and Eskin D G 2017 Numerical modelling of ultrasonic waves in a bubbly Newtonian liquid using a high-order acoustic cavitation model *Ultrason. Sonochem.* **37** 660–8
[7] Lebon G S B, Pericleous K, Tzanakis I and Eskin D 2016 A model of cavitation for the treatment of a moving liquid metal volume *Int. J. Cast Met. Res.* **29** 324–30
[8] Tzanakis I, Hodnett M, Lebon G S B, Dezhkunov N and Eskin D G 2016 Calibration and performance assessment of an innovative high-temperature cavitometer *Sens. Actuators Phys.* **240** 57–69
[9] Hurrell A M and Rajagopal S 2017 The Practicalities of Obtaining and Using Hydrophone Calibration Data to Derive Pressure Waveforms *IEEE Trans. Ultrason. Ferroelectr. Freq. Control* **64** 126–40
[10] Tzanakis I, Lebon G S B, Subroto T, Eskin D and Pericleous K 2019 Acoustic cavitation measurements and modeling in liquid aluminum *accepted for Light Metals2019*

[11] Lebon G S B, Tzanakis I, Pericleous K, Eskin D and Grant P S 2019 Ultrasonic liquid metal processing: The essential role of cavitation bubbles in controlling acoustic streaming *Ultrason. Sonochem.* doi.org/10.1016/j.ultsonch.2019.01.021
[12] Alba-Baena N and Eskin D 2016 Kinetics of Ultrasonic Degassing of Aluminum Alloys *Light Metals 2013* ed B A Sadler (Cham: Springer International Publishing) pp 957–62
[13] Atamanenko T V, Eskin D G, Sluiter M and Katgerman L 2011 On the mechanism of grain refinement in Al–Zr–Ti alloys *J. Alloys Compd.* **509** 57–60
[14] Zhang L 2013 *Ultrasonic processing of aluminium alloys* PhD Thesis (Delft University of Technology)